

A MIXED CONVECTION STUDY IN A HORIZONTAL CHANNEL

Paulo Mohallem Guimarães

UNIFEI – Universidade Federal de Itajubá – www.unifei.edu.br
paulomgui@uol.com.br

Márcio de Oliveira

UNIFEI – Universidade Federal de Itajubá – www.unifei.edu.br
maroli@iem.efei.br

Genésio José Menon

UNIFEI – Universidade Federal de Itajubá – www.unifei.edu.br
genesio@iem.efei.br

Abstract: *A study of a mixed convection flow in a backward facing-step heated from below is performed. At the entrance region, the flow has a fully developed parabolic velocity and a linear temperature profiles. The problem is considered to be laminar, bi-dimensional, incompressible, and under the unsteady regime. The conservation equations are solved through the finite element method using the four-noded quadrilateral element to calculate the distributions of the primitive variables U , V , P , and T . The Petrov-Galerkin approximation was used together with the Penalty formulation. Comparison with some results from the literature shows a good agreement with those performed by the techniques used in the present work. The Nusselt numbers for some cases are obtained by ranging the Froude number and the Reynolds number. A better comprehension of the flow in a such geometry and boundary conditions suggested in the paper is accomplished. Some expected flow effects are shown such as the increase of Nusselt number with the increase of Reynolds and Froude numbers. Not only is the behavior of the recirculation and thermal cells reasoned, but also their contribution to the heat transfer exchange as a whole.*

Key words: *Finite Element Method, Mixed Convection, Petrov-Galerkin.*

1. Introduction

The problem of laminar flow over backward-facing step geometries in natural, forced, and mixed convection has been investigated extensively, both numerically and experimentally. The reason for this is that the flow separation, reattachment, and recirculation which are influenced by a sudden change in flow geometry and by thermal conditions that are present, play an important role in the design of a wide range of heat transfer devices such as cooling systems for electronic equipment, combustion chambers, high performance heat exchangers, chemical process equipment, environmental control systems, and cooling passages in turbine blades.

A significant amount of fluid energy is involved in these problems and, then, affecting their heat transfer performance. Some investigations have dealt with similar problems and are mentioned here.

First, Lin et al (1991) studied the mixed convection heat transfer in inclined backward-facing step flows. The results presented indicate that for some convective flow conditions in backward-facing step geometry, buoyancy effects and/or inclination angle can play a significant role and should be included in the analysis.

More recently, the effect of the backward-facing step heights on turbulent mixed convection flow along a vertical flat plate is examined experimentally by Abu-Mulaweh et al (2002). The results reveal that the turbulence intensity of the streamwise and transverse velocity fluctuations and the intensity of temperature fluctuations downstream of the step increase as the step height increases.

Giovannini and Bortulus (1997) analyzed the heat transfer in the reattachment zone downstream of a backward facing step. It has been noticed that in recirculating flows the heat transfer coefficient, which is maximum in the reattachment zone, does not correspond in position with the mean reattachment point. The overall analysis shows the fundamental role played by the vortex structures concerning the mixing process and the heat transfer. Impact and sweeping mechanisms carry external cold fluid toward the heated solid wall and then ensure transport far away. These mechanisms determine the relative position of the reattachment and maximum heat transfer points both downstream and upstream.

The spatial-temporal movements of the reattachment and separation points in a 2-D backward-facing step flow with an oscillating bottom wall were characterized by Huteau et al (2000). The results also showed that both reattachment and separation points moved toward (away from) the step during upward (downward) motion of the wall, and that their rate of variation or the covered distance is a strong function of the wall oscillation.

Soong et al. (2001) investigated numerically the thermal-fluid behavior in a rectangular enclosure of width-to-height aspect ratio 4:1 heated from below with wall-temperature changing sinusoidally in time. The results demonstrated that a bottom-wall temperature modulation of larger amplitude and/or lower frequency generated a relative stability.

Finally, the onset condition of regular longitudinal vortex rolls in the thermal entrance region of plane Poiseuille flow heated from below was analyzed by Kim et al (2003). As expected, the critical position moves upstream as Rayleigh number increases and an increase in Reynolds number makes the system more stable.

In this paper, the study of a mixed convection flow in backward facing-step geometry is carried out. The flow is considered to be laminar, incompressible, and under the unsteady regime, although the results are presented in the steady regime. The channel entrance velocity profile is taken as parabolic and fully developed with no vertical components, and as for its temperature, the profile is linear. The geometrical parameters of the problem are not varied. Therefore, the analysis of the heat transfer is only due to the range of Reynolds and Froude numbers keeping air as the flow fluid.

For validation of the computational code and the method used, some known numerical and experimental results from the literature are taken to be contrasted with those obtained in the present work for both an isothermal flow in a backward facing-step geometry and a mixed convection Poiseuille plane flow. The numerical method used to solve the conservation equations is the finite element method with the Petrov-Galerkin's formulation as well as the Penalty technique. The spatial discretization is composed of four-noded quadrilateral elements.

Once the code and method are validated, some cases are studied by ranging the Froude number (1/75, 1/150, and 1/300) and the Reynolds number (10 and 20) keeping the Prandtl number $Pr = 0.7$. Therefore, the Grashof number goes from 7500 to 120000.

An analysis of the flow recirculation cells and of the thermal cells present along the channel is carried out. These cells behavior dictates the heat transfer exchange and hence the Nusselt number.

2. Problem description

Figure (1) shows the channel geometry to be studied and the problem boundary conditions. The origin of the axes is placed at the top of the step. H_d is taken as the downstream height, L as the length, H_u as the upstream height, and H as the step height. For all the cases studied in this work, the values of such geometrical parameters are $H_d = 1$, $H = H_u = 0.5$, and $L = 30$. The channel upper wall is cooled at a constant temperature T_c , while the bottom wall is heated at a constant temperature T_h . The step wall is taken to be isolated. The cases studied throughout this paper have the upper and bottom wall temperatures equal to 0 and 1, respectively. At the inlet, the channel flow has a fully developed parabolic velocity profile and a linear temperature profile. As for the open boundary conditions OBC, as the line integrals for pressure are discretized and retained in the weighted residuals formulation, there is no need to apply conditions at the open boundary. This procedure can be found in Heinrich and Pepper (1999).

It is studied in this paper the unsteady mixed convection by considering the flow to be laminar and incompressible. However, the results shown belong to the steady regime.

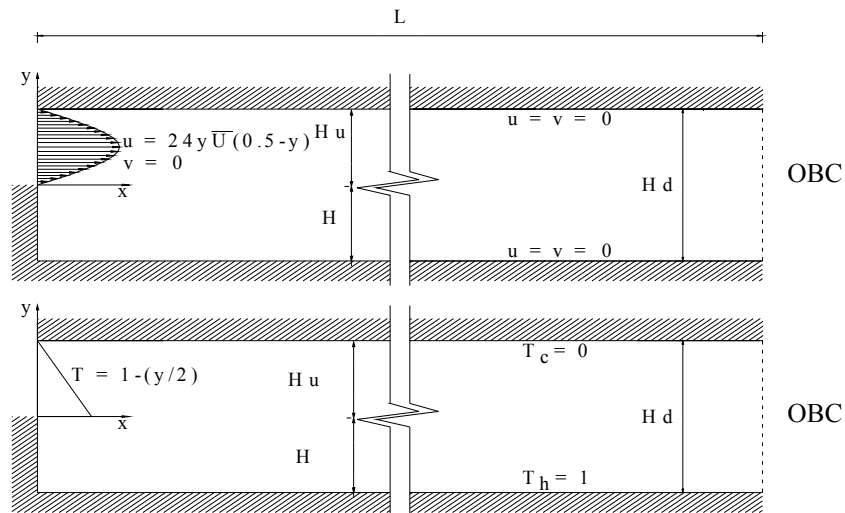


Figure 1. Channel geometry and boundary conditions.

3. Problem formulation

The problem governing equations are given by the equations of mass conservation, Navier-Stokes, and energy as follows:

$$\frac{\partial u}{\partial x} + \frac{\partial v}{\partial y} = 0 ; \quad (1)$$

$$\frac{\partial u}{\partial t'} + u \frac{\partial u}{\partial x} + v \frac{\partial u}{\partial y} = -\frac{1}{\rho_0} \frac{\partial p}{\partial x} + \nu \left(\frac{\partial^2 u}{\partial x^2} + \frac{\partial^2 u}{\partial y^2} \right); \quad (2)$$

$$\frac{\partial u}{\partial t'} + u \frac{\partial v}{\partial x} + v \frac{\partial v}{\partial y} = -\frac{1}{\rho_0} \frac{\partial p}{\partial y} + \nu \left(\frac{\partial^2 v}{\partial x^2} + \frac{\partial^2 v}{\partial y^2} \right) - g [1 + \beta_T (T - T_0)]; \quad (3)$$

$$\frac{\partial T}{\partial t'} + u \frac{\partial T}{\partial x} + v \frac{\partial T}{\partial y} = D_T \left(\frac{\partial^2 T}{\partial x^2} + \frac{\partial^2 T}{\partial y^2} \right); \quad (4)$$

where u and v are the velocity components, T is the fluid temperature, t' is the time field, D_T is the thermal diffusivity, β_T is the thermal expansion coefficient, ν is the kinematic viscosity, g is the gravitational acceleration, ρ_0 is the fluid density and T_0 is the reference temperature taken as $T_0 = T_c$.

Under the Boussinesq approximation and the following dimensionless parameters:

$$X = \frac{x}{L}; \quad Y = \frac{y}{L}; \quad U = \frac{u}{\bar{U}}; \quad V = \frac{v}{\bar{U}}; \quad P = \frac{p}{\rho_0 \bar{U}^2}; \quad t = \frac{t'}{(L/\bar{U})}; \quad \theta = (T - T_0)/\Delta T; \quad \Delta T = T_h - T_c; \quad (5)$$

$$Fr = \frac{Re^2}{Gr} = \frac{\bar{U}^2}{\beta_T g \Delta T L}; \quad Pr = \frac{\nu}{D_T}; \quad Gr = \frac{\beta_T g \Delta T L^3}{\nu^2}; \quad Re = \frac{\bar{U} \rho_0 L}{\mu};$$

which are named as the Froude number Fr , the Prandtl number Pr , the Grashof number Gr , the Reynolds number Re , the average velocity \bar{U} , and the dynamic viscosity μ , the dimensionless governing equations can be cast into the following form:

$$\frac{\partial U}{\partial X} + \frac{\partial V}{\partial Y} = 0; \quad (6)$$

$$\frac{\partial U}{\partial t} + U \frac{\partial U}{\partial X} + V \frac{\partial U}{\partial Y} = -\frac{\partial P}{\partial X} + \frac{1}{Re} \left(\frac{\partial^2 U}{\partial X^2} + \frac{\partial^2 U}{\partial Y^2} \right); \quad (7)$$

$$\frac{\partial V}{\partial t} + U \frac{\partial V}{\partial X} + V \frac{\partial V}{\partial Y} = -\frac{\partial P}{\partial Y} + \frac{1}{Re} \left(\frac{\partial^2 V}{\partial X^2} + \frac{\partial^2 V}{\partial Y^2} \right) + \frac{\theta}{Fr}; \quad (8)$$

$$\frac{\partial \theta}{\partial t} + U \frac{\partial \theta}{\partial X} + V \frac{\partial \theta}{\partial Y} = \frac{1}{Re Pr} \left(\frac{\partial^2 \theta}{\partial X^2} + \frac{\partial^2 \theta}{\partial Y^2} \right). \quad (9)$$

By applying the Petrov-Galerkin's formulation to the equations above, Eqs. (6) to (9), together with the Penalty technique, the following weak form of the conservation equations are:

$$\int_{\Omega} N_i \left[\frac{\partial U}{\partial t} + \frac{1}{Re} \left(\frac{\partial N_i}{\partial X} \frac{\partial U}{\partial X} + \frac{\partial N_i}{\partial Y} \frac{\partial U}{\partial Y} \right) \right] d\Omega + \int_{\Omega} \lambda \frac{\partial N_i}{\partial X} \left(\frac{\partial U}{\partial X} + \frac{\partial V}{\partial Y} \right) d\Omega = \int_{\Omega} (N_i + P_{i1}) \left(U \frac{\partial U}{\partial X} + V \frac{\partial U}{\partial Y} \right) d\Omega - \int_{\Gamma_0} N_i p n_x d\Gamma; \quad (10)$$

$$\int_{\Omega} N_i \left[\frac{\partial V}{\partial t} + \frac{1}{Re} \left(\frac{\partial N_i}{\partial X} \frac{\partial V}{\partial X} + \frac{\partial N_i}{\partial Y} \frac{\partial V}{\partial Y} \right) \right] d\Omega + \int_{\Omega} \lambda \frac{\partial N_i}{\partial Y} \left(\frac{\partial U}{\partial X} + \frac{\partial V}{\partial Y} \right) d\Omega = \int_{\Omega} \left[(N_i + P_{i1}) \left(U \frac{\partial V}{\partial X} + v \frac{\partial V}{\partial Y} \right) + N_i \frac{\theta}{Fr} \right] d\Omega - \int_{\Gamma_0} N_i p n_y d\Gamma; \quad (11)$$

$$\int_{\Omega} \left[N_i \frac{\partial \theta}{\partial t} + \frac{1}{Re Pr} \left(\frac{\partial N_i}{\partial X} \frac{\partial \theta}{\partial X} + \frac{\partial N_i}{\partial Y} \frac{\partial \theta}{\partial Y} \right) \right] d\Omega = \int_{\Omega} (N_i + P_{i2}) \left(u \frac{\partial \theta}{\partial x} + v \frac{\partial \theta}{\partial y} \right) d\Omega + \int_{\Gamma_1} N_i q d\Gamma; \quad (12)$$

where the dependent variables are approximated by:

$$U(X, Y, t) = \sum_j N_j(X, Y)U_j(t) ; \quad (13)$$

$$V(X, Y, t) = \sum_j N_j(X, Y)V_j(t) ; \quad (14)$$

$$\theta(X, Y, t) = \sum_j N_j(X, Y)\theta_j(t) ; \quad (15)$$

$$p(X, Y, t) = \sum_k M_k(X, Y)p_k(t) . \quad (16)$$

N_i and N_j denote the linear shape functions for U , V , and θ , and M_k denotes the shape functions for the constant piecewise pressure. P_{ij} are the Petrov-Galerkin perturbations applied to the convective terms only. These terms P_{ij} are defined as follows:

$$P_{ij} = k_j \left(U \frac{\partial N_i}{\partial X} + V \frac{\partial N_i}{\partial Y} \right); \quad (17)$$

$$\text{where: } k_j = \frac{\alpha_j \bar{h}}{|V|}; \quad \alpha_j = \coth \frac{\gamma_j}{2} - \frac{2}{\gamma_j}; \quad \gamma_j = \frac{|V| \bar{h}}{\varepsilon_j}; \quad (18)$$

and γ is the element Péclet number, $|V|$ is the absolute value of the velocity vector that represents the fluid average velocity within the each element, \bar{h} is the element average size, ε_j equals to $1/Re$, and λ is the Penalty parameter which is considered to be 10^9 . The time integration is by a semi-implicit backward Euler method. Moreover, the convective terms are calculated explicitly and the viscous and Penalty terms implicitly. The temperatures and velocities are interpolated by using the four-noded quadrilateral elements and the pressure by the one-noded one. Finally, the reduced integration is applied to the penalty term to avoid numerical locking.

The local Nusselt number is defined as:

$$Nu_L = - \frac{L}{(T_h - T_c)} \frac{\partial T}{\partial y} \Big|_S . \quad (19)$$

Substituting the dimensionless parameters Y and θ from Eqs. (5) into Eq. (19), the new expression for the local Nusselt number is:

$$Nu_L = - \frac{\partial \theta}{\partial y} \Big|_S . \quad (20)$$

For that being so, the average Nusselt number along a surface S can be written as:

$$Nu = - \frac{1}{S} \int_S \frac{\partial \theta}{\partial y} ds . \quad (21)$$

The algorithm is validated by comparing the results of the present work with both the ones obtained in experimental and numerical investigations. Figures (2) and (3) show the geometries and the boundary conditions used in the first and second comparisons, respectively. Again, OBC stands for open boundary conditions.

The first comparison is accomplished by using the experimental results presented by Lee and Mateescu (1998), and Armaly et al.(1983) and by the numerical ones achieved by Lee and Mateescu (1998), Gartling (1990), Kim and Moin (1985), and Sohn (1988). The air flow of the present comparison analysis is taken as bidimensional, laminar, incompressible, and under the unsteady regime. The domain is a horizontal upstream backward-facing step channel whose inlet has a fully developed velocity profile given by $u = 24y(0.5-y)\bar{U}$ and $v = 0$ in which $Re = 800$. The computational domain has $L = 30$, $Hd = 1$, and $Hu = Hd = 0.5$ where all walls are under the no-slip condition. The domain discretization is done by a structured mesh with 6000 elements, and spatial increments $\Delta x = 0.1$, $\Delta y = 0.05$, a time step $\Delta t = 0.05$, and 10000 iterations.

Table (1) shows the results from the first comparison for the flow separation distance X_s on the upper surface and its reattachment distance X_r . As for the bottom surface, the comparison is made on the reattachment distance X_r . As can be noticed, the results of the present work agree well with the ones from the experimental and numerical studies chosen.

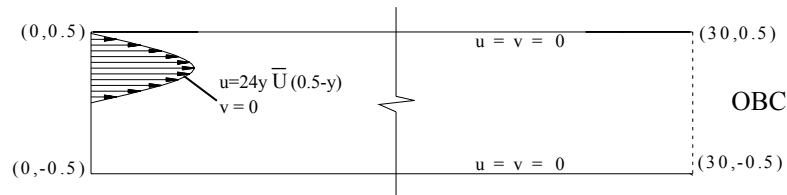


Figure 2. Geometry and boundary conditions for the first comparison.

Table 1. Comparison of computed predictions and experimental measurements of dimensionless lengths (with respect to H_d) of separation and reattachment on upper and lower walls.

Length on	Experimental results			Computed results			
	T.Lee and D.Mateescu (1998)	Armaly et al. (1983)	Present prediction	Gartling's prediction (1990)	Kim & Moin (1985)	T.Lee and D.Mateescu (1998)	Sohn (1988)
Lower Wall x_r	6.45	7.0	5.75	6.1	6.0	6.0	5.8
Upper Wall x_s	5.15	5.7	4.95	4.85	-	4.8	-
x_{rs}	10.25	10.0	9.9	10.48	-	10.3	-
$x_{rs}-x_s$	5.1	4.3	4.95	5.63	5.75	5.5	4.63
Reynolds	805	800	800	800	800	800	800
H_d/H_u	2	1.94	2	2	2	2	2

The second comparison is performed with the numerical results shown by Comini et al (1997). The contrasting study is carried out by considering a problem involving mixed convective heat transfer with the flow being bidimensional, laminar, and incompressible in the unsteady regime. In this case, some values are chosen such as $Re=10$, $Pr = 0.67$, and $Fr = 1/150$. The grid has 4000 quadrilateral four-noded elements with $\Delta x=0.1$, $\Delta y=0.15$, $\Delta t=0.01$ and 1000 iterations. Figure (4) displays the average Nusselt number on the upper surface versus time. After approximately iteration 500, the regime turns to be periodic with the average Nusselt number on the upper wall oscillating around a mean value of 2.44. This value agrees satisfactorily with the one found by Comini et al (1997) which is 2.34, resulting in a deviation of about 4%.

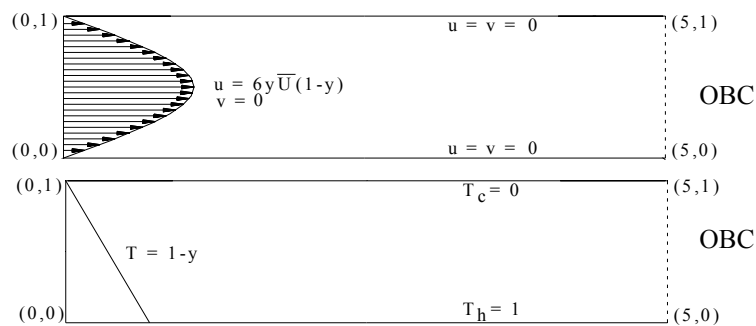


Figure 3. Geometry and boundary conditions for the second comparison.

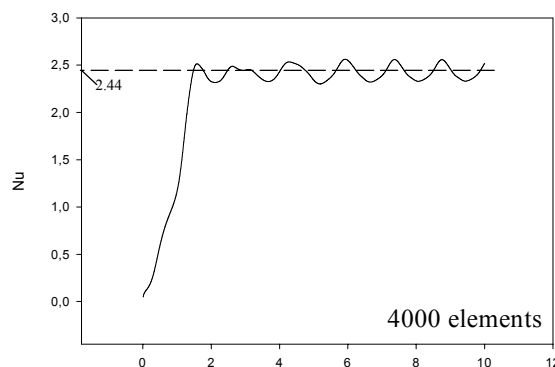


Figure 4. Average Nusselt number Nu along the upper surface versus time for a Poiseuille flow heated from below.

4. Results

Table (2) shows the non-dimensional parameters range for each case and the average Nusselt number found in each case. Such range is featured by taking the Froude number to be 1/75, 1/150, and 1/300, and, finally, the Reynolds number to be 10 and 20. For all cases, the Prandtl number is kept $Pr = 0.7$. Once the Froude and Reynolds numbers are chosen, the Grashof numbers are calculated and ranges between the values 7500 and 120000.

These cases are performed by taking different time steps, for instance, $\Delta t = 0.01$ (cases 1 and 2), $\Delta t = 0.005$ (cases 3 and 4), $\Delta t = 0.002$ (case 5) e $\Delta t = 0.0015$ (case 6), and different iteration numbers such as 10000 (cases 1 and 2), 14000 (case 3), 20000 (case 4), 65000 (case 5), and 75000 (case 6). Figure (5) presents the temperature distribution along the channel for all the cases from Table (2). It can be observed that the isotherms behave in a repeated way along the channel characterizing thermal cells that have their size larger as Re increases and Fr decreases. These thermal cell enlargements are related to a more intense heat exchange along the wall, as can be noticed in Fig. (5) and, hence, higher Nusselt numbers. This effect is clear in Fig. (6), where the average Nusselt number on the cold wall is plotted by ranging the Froude number and keeping $Re = 10$ and 20 for each set of cases, and $Pr = 0.7$ for all of them.

Table 2. Values of the parameters Fr , Re , Gr , and the average Nusselt number on the upper wall for the cases studied.

	Pr	Fr	Re	Gr	Nu
Case 1	0.7	1/75	10	7500	2.0485
Case 2	0.7	1/150	10	15000	2.4824
Case 3	0.7	1/300	10	30000	2.6981
Case 4	0.7	1/75	20	30000	2.8447
Case 5	0.7	1/150	20	60000	3.1655
Case 6	0.7	1/300	20	120000	3.2585

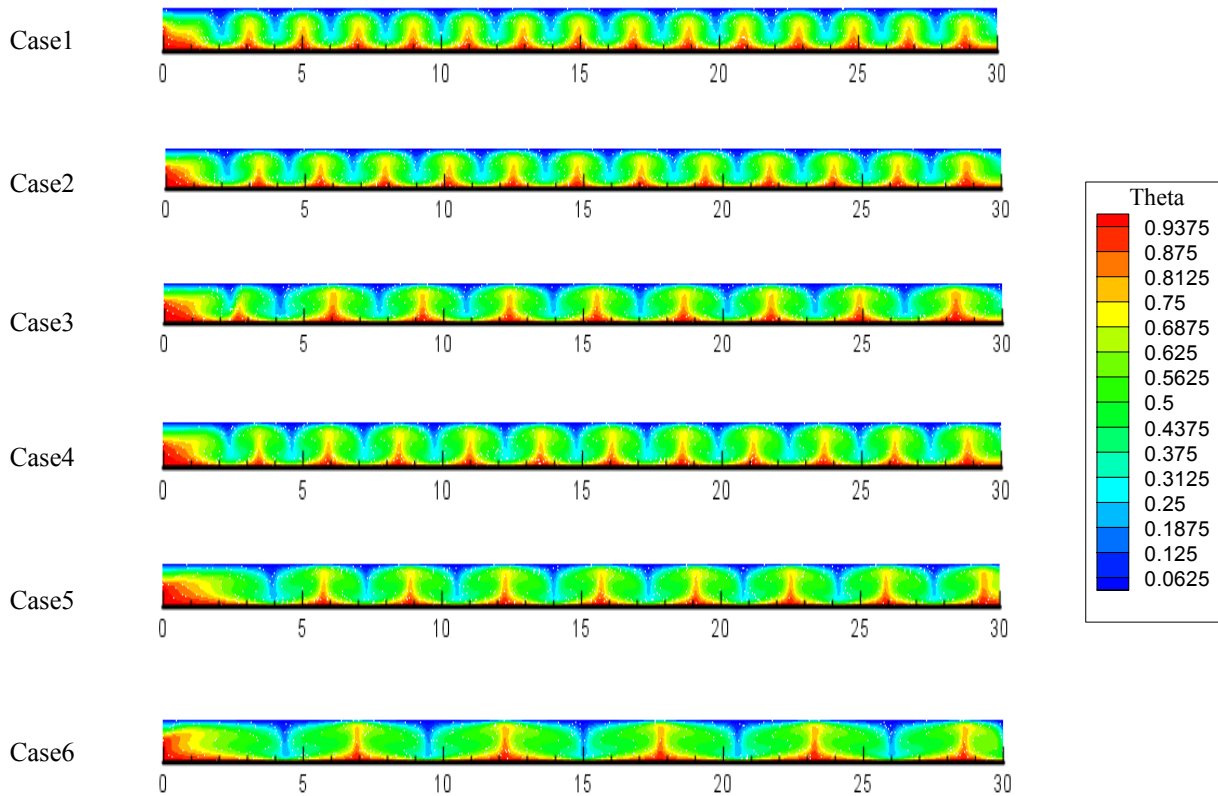


Figure 5. Temperature distribution along the channel with Fr , Re , and Gr ranging, respectively, from 1/75, 10, and 7500 to 1/300, 20, and 120000.

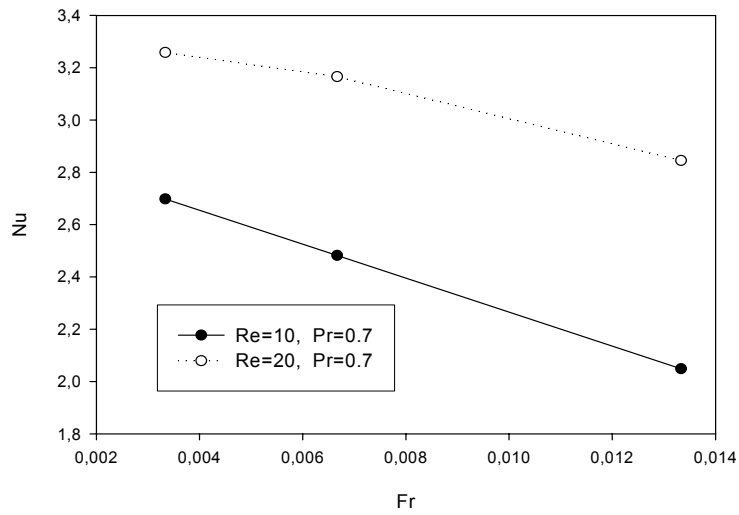


Figure 6. Average Nusselt number along the cold wall versus Froude number.

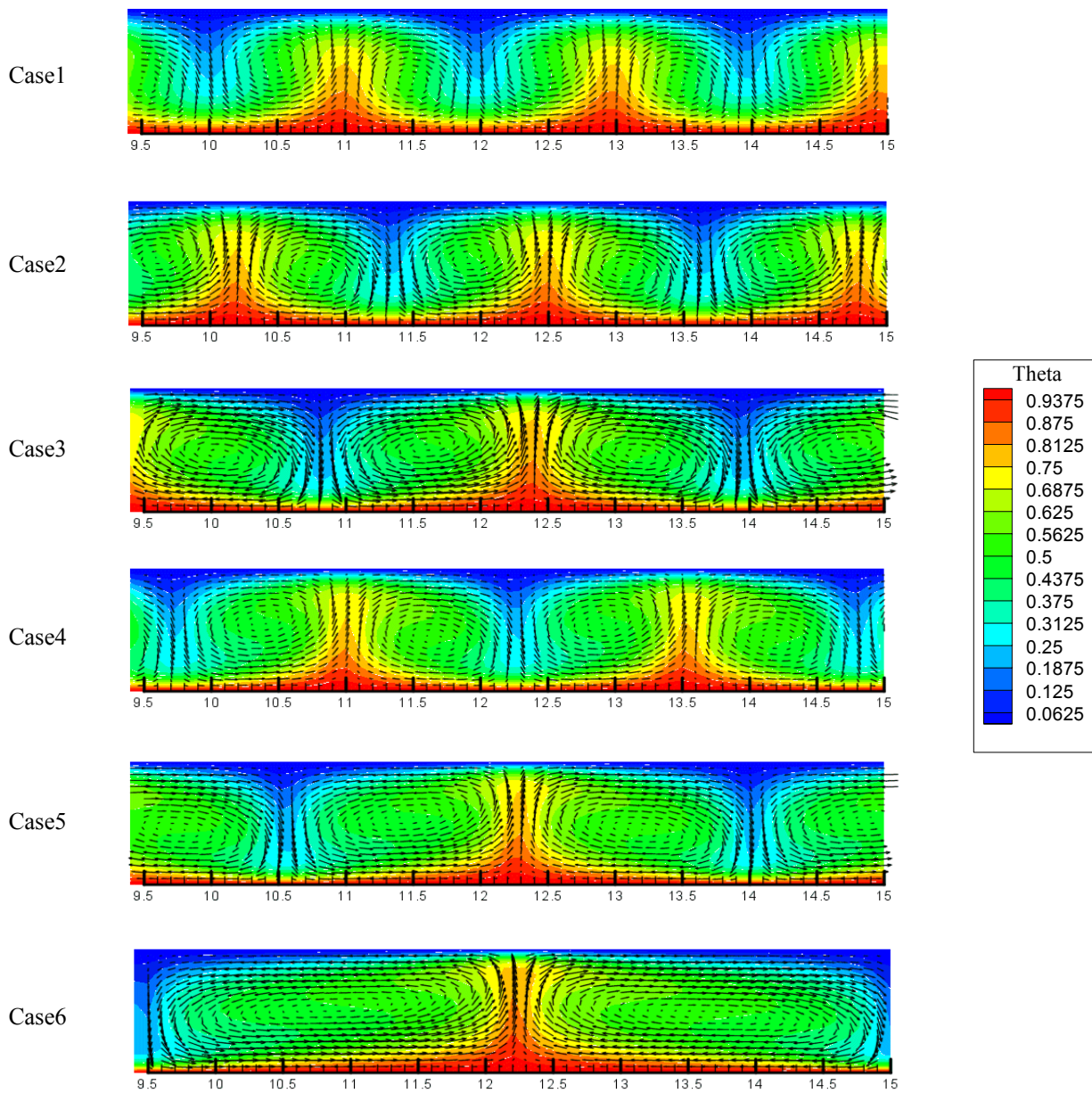


Figure 7. Velocity and temperature cells with Fr, Re, and Gr ranging, respectively, from 1/75, 10, and 7500 to 1/300, 20, and 120000. Just part of the length is shown here.

As mentioned before, it can be seen in Fig. (7) that the thermal cells get bigger as Fr decreases and Re increases. It can be observed clearly the closer approximations of the isotherms near the upper wall in each cell mean region. On the other hand, the same isotherm pattern is reached on the bottom wall but between two thermal cells. In these two regions, one can find bigger local temperature gradients, hence featuring higher local rates of heat transfer. It is noticed that in cases 1, 2, and 3 that as Fr decreases, the isotherms get even closer in the regions just mentioned before. The same thing happens for each pair of cases such as 1 - 4, 2 - 5, and 3 - 6. Taking as reference the recirculation cell size of case 1, the ones in cases 2 and 3 are 20% and 60% bigger, respectively. Moreover, if the recirculation cell size of case 4 is now taken as reference, the ones in cases 5 and 6 are about 55% and 145% larger, respectively. Such behavior is also found to be true for the thermal cells. Noticeably, case 6 is the one that brings the highest Nusselt number featuring its main flow giving place to the secondary flow. The recirculation cells expand horizontally and vertically forcing the main flow to pass through smaller passages. Then, flow is remarkably featured by the recirculation. Although it is not shown here and also being subject of future researches, it is important to mention the fact that the fluid flow development is characterized by the recirculation cells rolling downstream the channel.

Figure (8) pictures the average Nusselt number along the upper and bottom surfaces for the case 5, where $Fr = 1/50$, $Re = 20$, and $Pr = 0.7$. This case is performed by taking 100000 iterations with a time step $\Delta t = 0.002$. The periodic regime is reached when t is around 65. It is highlighted that each behavior follows the same pattern and that the mean values for each curve is close to each other around the value of 3.2.

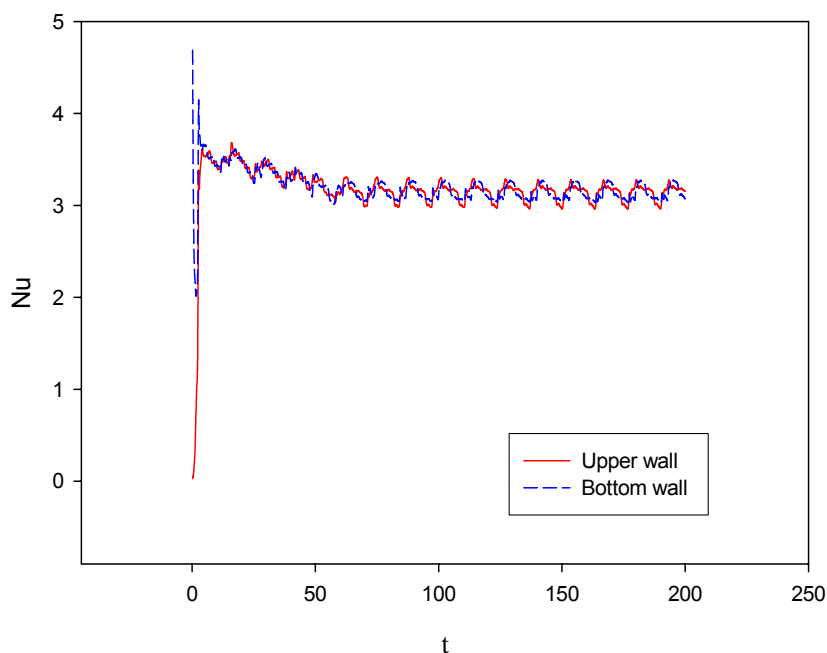


Figure 8. Average Nusselt number Nu measured along the upper and bottom surfaces versus time for the case 5.

5. Conclusions

In this work it is studied the mixed convection heat transfer in a backward facing-step heated from below. The flow is considered to be laminar and incompressible in the unsteady regime, although the results are presented in the steady regime. At the inlet, the flow has a fully developed parabolic velocity profile and a linear temperature variation. It was verified the influence of Froude number (1/75, 1/150, 1/300) and Reynolds number (10 and 20) on the process by keeping $Pr = 0.7$ throughout the study. For all the cases studied, a grid having 6000 four-noded elements was used to discretize the computational domain. The numerical method used was the Petrov-Galerkin with the Penalty formulation. As expected, the Nusselt number increased as Reynolds number increased. For the most critical case, number 6, where $Fr = 1/300$, $Re = 20$, and $Gr = 60000$, the heat transfer flow was mainly characterized by stronger recirculation cells. Both the thermal and recirculation cell sizes for the case 3 ($Fr = 1/300$, $Re = 10$, $Gr = 30000$) and case 6 ($Fr = 1/300$, $Re = 20$, $Gr = 120000$) had their sizes increased for more than 100% according to their references cases such as case 1 (1/75, $Re=10$, $Gr = 7500$) and case 4 (1/75, $Re = 20$, $Gr = 30000$), respectively.

6. Acknowledgements

The authors acknowledge CAPES for its financial support without which this work would be not be possible.

7. References

Abu-Mulaweh, H. I., Chen T. S., and Armaly B. F., 2002, "Turbulent Mixed Convection Flow Over a Backward-Facing Step – The Effect of the step Heights", *International Journal of Heat and Fluid Flow*, Vol. 23, pp. 758-765.

- Armaly, B. F., Durst, F., Pereira, and J. C. F. & Schonung, B., 1983, "Experimental and Theoretical Investigation of Backward-Facing Step Flow", *Journal of Fluid Mechanics*, Vol. 127, pp. 473-496.
- Comini, G., Manzan M., and Cortella G., 1997, "Open Boundary Conditions for the Streamfunction - Vorticity Formulation of Unsteady Laminar Convection", *Numerical Heat Transfer, Part B*, Vol. 31, pp. 217-234.
- Gartling, D. K., 1990, "A Test Problem for Outflow Boundary Conditions – Flow over a Backward-Facing Step", *International Journal of Numerical Methods in Fluids*, Vol. 11, pp. 953-967.
- Giovannini A. and Bortolus M. V., 1997, "Transfert de Chaleur au Voisinage du Point de Recollement en Aval d'une Marche Descendante", *Rev Gén Therm*, Vol. 37, pp. 89-102.
- Heinrich, J. C. and Pepper, D W., 1999, "Intermediate Finite Element Method", Ed Taylor & Francis, USA.
- Huteau F., Lee T. and Mateescu D., 2000, "Past a 2-D Backward-Facing Step with an Oscillating Wall", *Journal of Fluids and Structures*, Vol. 14, pp. 691-696.
- Kim, C. M., Chung T. J., and Choi C. K., 2003, "The Onset of Convective Instability in the Thermal Entrance Region of Plane Poiseuille Flow Heated Uniformly from Below", *International Journal of Heat and Mass Transfer*, Vol.46, pp. 2629-2636.
- Kim, J. and Moin, P., 1985, "Application of a Fractional-Step Method to Incompressible Navier - Stokes Equations", *Journal of Computational Physics*, Vol. 59, pp. 308-323.
- Lee, T. and Mateescu, D., 1998, "Experimental and Numerical Investigation of 2-D Backward - Facing Step Flow", *Journal of Fluids and Structures*, Vol. 12, pp. 703-716.
- Numerical Methods in Fluids, Vol. 8, pp. 1469-1490.
- Lin, J. T., Armaly B. F., and Chen T. S., 1991, "Mixed Convection Heat Transfer in Inclined Backward-Facing Step Flows", *International Journal of Heat and Mass Transfer*, Vol. 34, No. 6, pp. 1568-1571.
- Sohn, J., 1988, "Evaluation of FIDAP on Some Classical Laminar and Turbulent Benchmarks", *International Journal of Numerical Methods in Fluids*, Vol. 8, pp. 1469-1490.
- Soong, C. Y., Tzeng P. Y., and Hsieh C. D., 2001, "Numerical Study of Bottom-Wall Temperature Modulation Effects on Thermal Instability and Oscillatory Cellular Convection in Rectangular Enclosure", *International Journal of Heat and Mass Transfer*, Vol. 44, pp. 3855-3868.